LA-UR-73-968

TITLE: Prompt and Delayed Neutron Yields from Low Energy Photofission of ^{232}Th, ^{235}U, ^{238}U, and ^{239}Pu.

AUTHOR(S): John T. Caldwell
Edward J. Dowdy
Gary M. Worth

SUBMITTED TO: Talk for the IAEA Symposium on the Physics and Chemistry of Fission. (To be published by the IAEA)

los alamos
scientific laboratory
of the University of California
LOS ALAMOS, NEW MEXICO 87544

Form No. 836
St. No. 2629
1/73

UNITED STATES
ATOMIC ENERGY COMMISSION
CONTRACT W-7405-ENG. 36

Prompt and Delayed Neutron Yields from Low Energy Photofission of ^{232}Th, ^{235}U, ^{238}U, and ^{239}Pu

John T. Caldwell
Edward J. Dowdy
Gary M. Worth

Los Alamos Scientific Laboratory
University of California
P. O. Box 1663
Los Alamos, New Mexico 87544, USA

Prompt and Delayed Neutron Yields from Low Energy Photofission of ^{232}Th, ^{235}U, ^{238}U, and ^{239}Pu

1. INTRODUCTION

There have been only a few previous measurements [1-3] of $\bar{\nu}_p$, the mean number of prompt neutrons emitted per fission event, for photofission of the major fissionable isotopes at low energies, and no previous measurement of the dependence of $\bar{\nu}_p$ on photoexcitation energy. We find only one report [4] of measurements of the absolute delayed neutron fractions, β, for photofission. A somewhat larger body of information [5-7] is available on the determination of the competition between neutron emission and fission for photoexcitation, made possible through measurements of $\langle \Gamma_n/\Gamma_f \rangle$, the average ratio of the neutron emission width to the fission width. There have been no previous simultaneous measurements of these quantities.

Values of these parameters are useful in establishing or confirming fission systematics for expanding our understanding of the fission process and in interpreting the results of measurements of dependent quantities such as the partial cross sections.

In this paper, we report on the simultaneous measurement, using a single detector, of $\bar{\nu}_p$, β, and $\langle \Gamma_n/\Gamma_f \rangle$ for photoexcitation of ^{232}Th, ^{235}U, ^{238}U, ^{239}Pu using electron bremsstrahlung from 8-, 10-, 10.2-, and 12-MeV electrons.

2. EXPERIMENTAL METHOD

2.1 Irradiation

Electrons were accelerated to the appropriate energy in 10 nsec pulses with a repetition rate of 360 pps in the USAEC Electron Linear Accelerator in Santa Barbara, Ca., operated by EG&G, Inc. Conversion to bremsstrahlung took place in a 10 cm cube of aluminum. The bremsstrahlung in the forward direction was collimated to a 2.5 cm diameter beam using a 20 cm thick iron collimator. Samples of fissionable material, described in Table I, were placed at the center of the detector shown in Fig. 1, with the detector axis aligned with the beam. The sample to converter distance was approximately 1 meter. The electron beam currents were monitored using the converter as a Faraday cup. The detector was shielded on all sides with borated polythene blocks, and materials with low (γ,n) reaction thresholds were excluded from the vicinity of the converter. Machine-generated backgrounds were determined by irradiating an aluminum disk in the sample position.

Table I

Fissionable Material Sample Description

Sample	Physical Description	Isotopic Analysis
^{232}Th	Disk, 5 cm diameter, 76 grams	100% Th-232
^{235}U	Disk, 5 cm diameter, 20 grams	1.0% U-234 93.23% U-235 0.36% U-236 5.41% U-238
^{238}U	Disk, 5 cm diameter, 58.6 grams	0.02% U-235 99.98% U-238
^{239}Pu	Disk, 2.29 cm diameter, 4.98 grams Ni canned	≤ 0.004% Pu-238 97.67% Pu-239 2.28% Pu-240 0.048% Pu-241 0.002% Pu-242

2.2 Neutron Detection System

The detection system has been described in detail elsewhere [8]. The neutron detector was a polythene cube, 61 cm on a side, containing fifty-three ^{3}He proportional counter tubes (in four concentric rings), each 2.54 cm diameter and 61 cm long, with filling pressures of 6-, 4-, 4-, and 3-atmospheres for the innermost-to-outermost ring of tubes, respectively. Neutrons generated in photoreactions in the samples were moderated in the polythene and captured with high probability in the ^{3}He tubes. The efficiency for detecting the prompt neutrons from the spontaneous fission of ^{252}Cf was measured to be 52%, assuming $\bar{\nu}_p = 3.784$, and the efficiency as a function of neutron energy has been calculated using Monte Carlo techniques.

The neutron slowing down process and the increased probability of capture at lower energies produced a broad capture time distribution with a distinct "dieaway" time for each ring of ^{3}He tubes. This distribution in time allowed for the detection of prompt neutrons with high efficiency even though the detection system was paralyzed during the gamma flash, and for a few μsec thereafter.

The pulses from the ^{3}He tubes were processed as indicated in Fig. 2. Each ring of tubes had common high voltage and amplification modules, and the amplified pulses were presented to discriminators, set to fire at voltages just above the noise level. The standard slow logic pulses from the discriminators were routed to a logic OR module, and the OR output line served as the data path. The pulses from the OR module were routed to a LASL-designed unit identified as a multiplicity sorter, and also to a multichannel scaler and a delayed neutron scaler. The multichannel scaler was used to record the time dependence of pulses from the neutron detector following a trigger derived from the linac. The delayed neutron scaler was used to scale the pulses from the detector following the dieaway of the prompt neutrons. The multiplicity sorter, described in detail elsewhere [9], is basically a digital-to-analog converter with a variable count gate width. Pulses appearing at the input following the linac-derived count gate trigger are scaled and the output pulse height is uniquely determined by the number (up to 9) of pulses arriving during the count gate. The pulse height analyzed output of the multiplicity sorter provided the measured multiplicity distribution.

With the linac pulse repetition rate of 360 pps, the time between pulses was 2778 μsec, and the prompt neutron population was negligible beyond 1200 μsec. So, the prompt neutrons were detected in a count gate opening a few microseconds after the gamma flash and closing at a variable time (usually 500 μsec) after that. The delayed neutrons were detected in a time window opening at 1200 μsec and closing before the next linac pulse. The time history of pulses from the neutron detector obtained from a typical run is shown in Fig. 4 .

3. DATA REDUCTION

3.1 $\bar{\nu}_p$ Determination

Terrell [10] first demonstrated with an analytical derivation and a comparison with a large body of experimental data that the emitted prompt fission neutron multiplicity distribution $\{\rho_\nu\}$ can be described with the expression

$$\sum_{o}^{\nu} \rho_\nu = \tfrac{1}{2} + \tfrac{1}{2} f\left[\left(\frac{\nu - \bar{\nu}_p + \tfrac{1}{2} + b}{\sigma}\right)\right] \quad . \qquad (1)$$

where

$$f(x) = \frac{1}{\sqrt{2\pi}} \int_{-x}^{x} e^{-\frac{t^2}{2}} dt \quad . \qquad (2)$$

Here $\bar{\nu}_p$ is the average number of prompt neutrons emitted per fission, σ is a distribution width parameter, and

$$b \lesssim 0.01 \cong \tfrac{1}{2} - \tfrac{1}{2} f\left[\left(\frac{\bar{\nu}_p + \tfrac{1}{2}}{\sigma}\right)\right] \quad . \qquad (3)$$

Thus the $\{\rho_\nu\}$ distribution is a function only of the two parameters $\bar{\nu}_p$ and σ.

Consideration of the effects of non-unity detector efficiency leads to the following expression for the observed multiplicity distribution $\{P_\nu\}$:

$$P_\nu = \epsilon^\nu \sum_{n=\nu}^{N} \left(\frac{n!(1-\epsilon)^{n-\nu}}{\nu!(n-\nu)!}\right) \rho_n \quad . \qquad (4)$$

This expression is valid after the observed data has been corrected for background, pulse pileup, and deadtime effects. Here ρ_n is the emitted multiplicity of order n as determined

from Eq. (1), ϵ is the detector efficiency and N is the maximum order emitted multiplicity, usually taken to be 9. Since ϵ varies slightly with neutron energy, a small correction is made by using Terrell's approximate expression

$$\langle E \rangle \cong 0.74 + 0.653\ (\bar{\nu}_p + 1)^{\frac{1}{2}} \quad . \qquad (5)$$

The magnitude of the efficiency correction is about 2% between $\bar{\nu}_p = 3.784$ and $\bar{\nu}_p = 2.50$.

As can be seen from Eq. (4) the shape of the observed multiplicity distribution $\{P_\nu\}$ is a fairly sensitive function of $\bar{\nu}_p$ and σ. This is demonstrated in Fig. 3 which shows the ratios P_3/P_2 and P_4/P_2 as a function of $\bar{\nu}_p$ for $\sigma = 1.15$ and for a typical value of ϵ. For a given isotope and excitation energy $\bar{\nu}_p$ was actually determined by performing a weighted least squares fit of the observed multiplicity data of all orders ≥ 2 to Eq. (4) as a function of $\bar{\nu}_p$, σ. Since only bremsstrahlung energies of 12 MeV or less were used $(\gamma, 2n)$ reactions in all isotopes were negligible and thus all observed net $\geq$ order 2 events were uniquely associated with a fission event.

Since a fairly narrow range of excitation energies was covered it was felt that the width parameter σ for a given isotope should be essentially constant. This was found to be the case within the statistical accuracy of the data. Thus, an average value of σ for each isotope (different for each of the four isotopes) was determined and $\bar{\nu}_p$ at each excitation energy found from a one parameter least squares fit. The overall statistical error in $\bar{\nu}_p$ as determined in this fashion ranged between 0.07 and 0.14.

3.2 $\langle \Gamma_n / \Gamma_f \rangle$ Determination

Once $\bar{\nu}_p$ and σ were determined from the multiplicity shape distribution, Eq. (4) was used to determine a fission detection efficiency for the experimental quantity

$$\sum_{2}^{N} P_\nu \quad .$$

This served to determine the number of fission events occurring in a given run. Equation (4) was then also used to calculate the number of singles events due to photofission. This enabled us to determine from the total observed singles events and the singles background the number of singles due to (γ,n) reactions only and thus to determine the quantity $\langle \Gamma_n/\Gamma_f \rangle$. The overall experimental error in $\langle \Gamma_n/\Gamma_f \rangle$ was generally in the range of 5 to 10 percent.

3.3 Delayed Neutron Fraction

The delayed neutron fraction β was obtained by counting between beam bursts but after prompt dieaway. A typical time history of this data is shown in Fig. 3. This measurement was generally done simultaneously with the neutron multiplicity measurements. To improve statistical accuracy some high beam intensity delayed neutron runs were also made, notably for the Pu samples. For these runs the number of fission events was determined by scaling the prompt part of the dieaway between high and low intensity runs. Some data utilizing the "ring ratio spectrometer" [11] technique were also taken to determine the average energy of photofission delayed neutrons and thus a suitable ϵ. The overall experimental error in β ranged between 5 and 10 percent.

3.4 Further Corrections and Errors

Where warranted, corrections for the presence of minor isotopes have been made. This correction was most notable for the case of β for the ^{235}U sample and amounted to about 10 percent. Generally speaking the largest source of error in all quantities is the uncertainty generated by the error in $\langle \sigma_{^{232}Th} \rangle$. This error was approximately $\pm$ 0.05 for ^{235}U, ^{238}U, and ^{232}Th and $\pm$ 0.10 for ^{239}Pu and derives from the quality of the multiplicity shape distribution fit to the data.

4. RESULTS

4.1 $\bar{\nu}_p$

The values of $\bar{\nu}_p$ determined from this experiment are given in Table II. Included in Table II are the expected values of $\bar{\nu}_p$ as calculated from the expressions contained in the evaluations of Davey [12] for neutron induced fission of ^{234}U, ^{237}U, and ^{238}Pu and from the equation provided by Tu and Prince [13] for neutron induced fission of ^{231}Th. These expressions are:

Table II

$\bar{\nu}_p$ Values

Electron Energy, MeV	^{232}Th Meas.	Calc.[13]	^{235}U Meas.	Calc.[12]	^{238}U Meas.	Calc.[12]	^{239}Pu Meas.	Calc.[12]
8	1.963±0.108	2.13	2.456±0.086	2.55	2.457±0.088	2.48	---------	3.09
10	1.891±0.111	----	2.697±0.081	2.71	2.628±0.083	2.65	3.32±0.08	3.25
10.2	1.891±0.111	----	2.612±0.079	----	2.585±0.082	----	3.17±0.14	----
12	2.084±0.107	----	2.963±0.072	2.91	2.802±0.078	2.85	3.43±0.10	3.46

$$\bar{\nu}_p \text{ (E)} = 2.352 + 0.1349E \text{ for } ^{234}U + n$$

$$\bar{\nu}_p \text{ (E)} = 2.386 + 0.1412E \text{ for } ^{237}U + n$$

$$\bar{\nu}_p \text{ (E)} = 2.914 + 0.1436E \text{ for } ^{239}Pu + n$$

and $$\bar{\nu}_p = 2.13 \text{ for } ^{231}Th + n_{th}$$

To calculate the $\bar{\nu}_p$ values to compare with our measured values, the excitation energies in these expressions were taken as the difference between the average photoexcitation energies and the neutron separation energies for the compound nuclei. The average photoexcitation energies were calculated as

$$\langle E_\gamma \rangle = \frac{\int_0^\infty E\ \sigma_{\gamma,f}(E)\ x(E)\ dE}{\int_0^\infty \sigma_{\gamma,f}(E)\ x(E)\ dE}$$

where $x(E)$ is the bremsstrahlung spectrum as given by Sandifer [14] and $\sigma_{\gamma,f}(E)$ are the differential photofission cross-sections for the appropriate target nuclei [6,15-18]. These average photoexcitation energies were very nearly the same for all the nuclei studied, being 6.80-, 7.99-, and 9.44-MeV for electron energies of 8-, 10-, and 12-MeV.respectively.

The agreement among the measured values and those calculated from the evaluations is exceptionally good. Assuming linear dependence of $\bar{\nu}_p$ on photoexcitation energy for our data results in the following expressions obtained from least squares analyses:

$$\bar{\nu}_p (\langle E_\gamma \rangle) = 1.595 + 0.0449 \langle E_\gamma \rangle \text{ for } ^{232}Th \text{ with a correlation coefficient of } 0.557$$

$$\bar{\nu}_p (\langle E_\gamma \rangle) = 1.215 + 0.1819 \langle E_\gamma \rangle \text{ for } ^{235}U \text{ with a correlation coefficient of } 0.967$$

$$\bar{\nu}_p (\langle E_\gamma \rangle) = 1.619 + 0.1240 \langle E_\gamma \rangle \text{ for } ^{238}U \text{ with a correlation coefficient of } 0.981$$

$$\bar{\nu}_p (\langle E_\gamma \rangle) = 2.248 + 0.1244 \langle E_\gamma \rangle \text{ for } ^{239}Pu \text{ with a correlation coefficient of } 0.826.$$

It appears that a linear dependence is consistent with our data except for the ^{232}Th values. Previous evaluations [12,19] have noted a deviation from a single straight line fit for neutron induced fission of ^{232}Th and ^{233}U at low energies, and it is plausible that similar behavior might be found for the ^{232}Th compound nucleus.

4.2 β

The β values determined from this experiment are given in Table III, along with the data of Nikotin and Petrzhak [4] and the calculated values of Keepin [20]. The agreement between the values obtained by Nikotin and Petrzhak for 15 MeV electron bremsstrahlung and our weighted average is quite good. Keepin's correlation, however, requires higher values than the measured ones for all the nuclei except ^{235}U.

4.3 $\langle \Gamma_n/\Gamma_f \rangle$

The values of $\langle \Gamma_n/\Gamma_f \rangle$ obtained in the analysis of our experimental data are given in Table IV. We find strong dependence on excitation energy as have other recent investigators [6]. Their value for the ratio at the highest excitation energy for ^{238}U is consistent with ours, but their reported value of $\langle \Gamma_n/\Gamma_f \rangle = 18.5$ for ^{232}Th is considerably different from ours. They assumed values for $\bar{\nu}_p$ and their assumed value for ^{232}Th was higher than our measured value, but a re-analysis of their data with our measured $\bar{\nu}_p$ value reduces the value for the ratio to $\simeq 12$, still much larger than our measured value. Our ^{232}Th value gives a qualitatively better fit to the Z^2/A correlation of Huizenga and Vandenbosch [5]. Mafra, et al, [7] also reported some evidence of an energy dependence for the ratio $\langle \Gamma_n/\Gamma_f \rangle$ for ^{232}Th and ^{238}U. Their data were analyzed on the assumption of a constant $\bar{\nu}_p = 2.5$ for both nuclei, and we have made no re-analysis of their data with our measured $\bar{\nu}_p$ values.

Included in Table IV are the values for the ratio calculated using the empirical fit of Sikkeland, et al, [21]. Again, the value for ^{232}Th at the highest excitation energy represents a large deviation from the expected.

Table III

$\bar{\sigma}$ Values

Electron Energy, MeV	^{232}Th	^{235}U	^{238}U	^{239}Pu
8	0.0310±0.0027	0.0090±0.0008	0.0306±0.0024	----------
10	0.0306±0.0030	0.0088±0.0008	0.0276±0.0017	----------
10.2	0.0267±0.0016	0.0113±0.0007	0.0306±0.0014	0.00371±0.00017
12	0.0259±0.0031	0.0112±0.0008	0.0275±0.0019	0.00375±0.00022
Average ($1/\sigma^2$ weighted)	0.0280±0.0012	0.0102±0.0004	0.0291±0.0009	0.00372±0.00013
Previous Measurement [4]	0.038 ±0.006	0.0096±0.0013	0.031 ±0.004	0.0036 ±0.0006
Correlation Value [20]	0.0309	0.0101	0.0309	0.0043

Table IV

$\langle \Gamma_n/\Gamma_f \rangle$ Values

Electron Energy, MeV	^{232}Th	^{235}U	^{238}U	^{239}Pu
8	1.05±0.12	0.98±0.10	1.65±0.12	---------
10	3.77±0.32	1.06±0.09	2.59±0.14	---------
10.2	3.56±0.32	1.09±0.09	2.608±0.147	0.29±0.08
12	6.28±0.48	1.18±0.08	2.89±0.14	1.02±0.08
Correlation Value [21]	3.16	1.22	3.22	0.65

REFERENCES

1. LAZAREVA, L.E., GAVRILOV, B.I., VALUEV, B.N., ZATSEPINA, G.N., STAVINSKY, V.S., Conference of the Academy of Sciences of the U.S.S.R. on the Peaceful Uses of Atomic Energy (1955) 217.

2. PROKHOROVA, L.I., SMIRENKIN, G.N., Atomnaya Énergiya 8 (1960) 457.

3. CONDÉ, H., HOLMBERG, M., Proceedings of the Symposium on the Physics and Chemistry of Fission II (1965) 57.

4. NIKOTIN, O.P., PETRZHAK, K.A., Atomnaya Énergiya 20 (1966) 268.

5. HUIZENGA J.R., VANDENBOSCH, R., in Nuclear Reactions edited by P.M. Endt and P.B. Smith II (1962) 42.

6. VEYSSIERE, A., BEIL, H., BERGERE, R., CARLOS, P., LEPRETRE, A., Nucl. Phys. A199 (1973) 45.

7. MAFRA, O.Y., KUNIYOSHI, S., GOLDEMBERG, J., Nucl. Phys. A186 (1972) 110.

8. DOWDY, E.J., CALDWELL, J.T., WORTH, G.M., to be published.

9. WORTH, G.M., CALDWELL, J.T., DOWDY, E.J., to be published.

10. TERRELL, J., Phys. Rev. 108 (1957) 783.

11. CALDWELL J.T., UCRL-50287 (1967).

12. DAVEY, W.G , Nucl. Sci. & Engng. 44 (1971) 345.

13. TU, PING-SHIU, PRINCE, A., J. Nucl. Energy 25 (1971) 599.

14. SANDIFER, C.W., EG&G, Inc., Santa Barbara, CA, private communication.

15. BOWMAN, C.D., AUCHAMPAUGH, G.F., FULTZ, S.C., Phys. Rev. 133 (1964) B676.

16. KHAN, A.M., KNOWLES, J.W., Nucl. Phys. A179 (1972) 333.

17. SHAPIRO, A., STUBBINS, W.F., Nucl. Sci. & Engng. 45 (1971) 47.

18. KATZ, L., BAERG, A.P., BROWN, F., Proc. of Conference on Peaceful Uses of Atomic Energy (1958) P/200.

19. FILLMORE, F.L., J. Nucl. Energy 22 (1968) 79.

20. KEEPIN, G.R., Physics of Nuclear Kinetics, Addison Wesley (1965) 101.

21. SIKKELAND, T., GHIORSO, A., NURMIA, M.J., Phys. Rev. 172 (1968) 1232.

FIGURE CAPTIONS

Fig. 1 The Neutron Detector. A 61 cm cube of polythene with four rings of 2.54 cm diameter, 61 cm long ^{3}He proportional counter tubes, and a central sample hole. The hole is 3.8 cm in radius, and the tubes are in rings with radii of 6.4-, 10.8-, 14.6-, and 17.8-cm. Fifty-three ^{3}He tubes were used in the work described in this paper.

Fig. 2 Block diagram of the Neutron Detection System.

Fig. 3 Typical variation of the ratios of observed multiplicities with $\bar{\nu}_p$ with $\sigma = 1.15$ and a typical efficiency.

Fig. 4 Time variation of pulses from the Neutron Detector during a typical run.

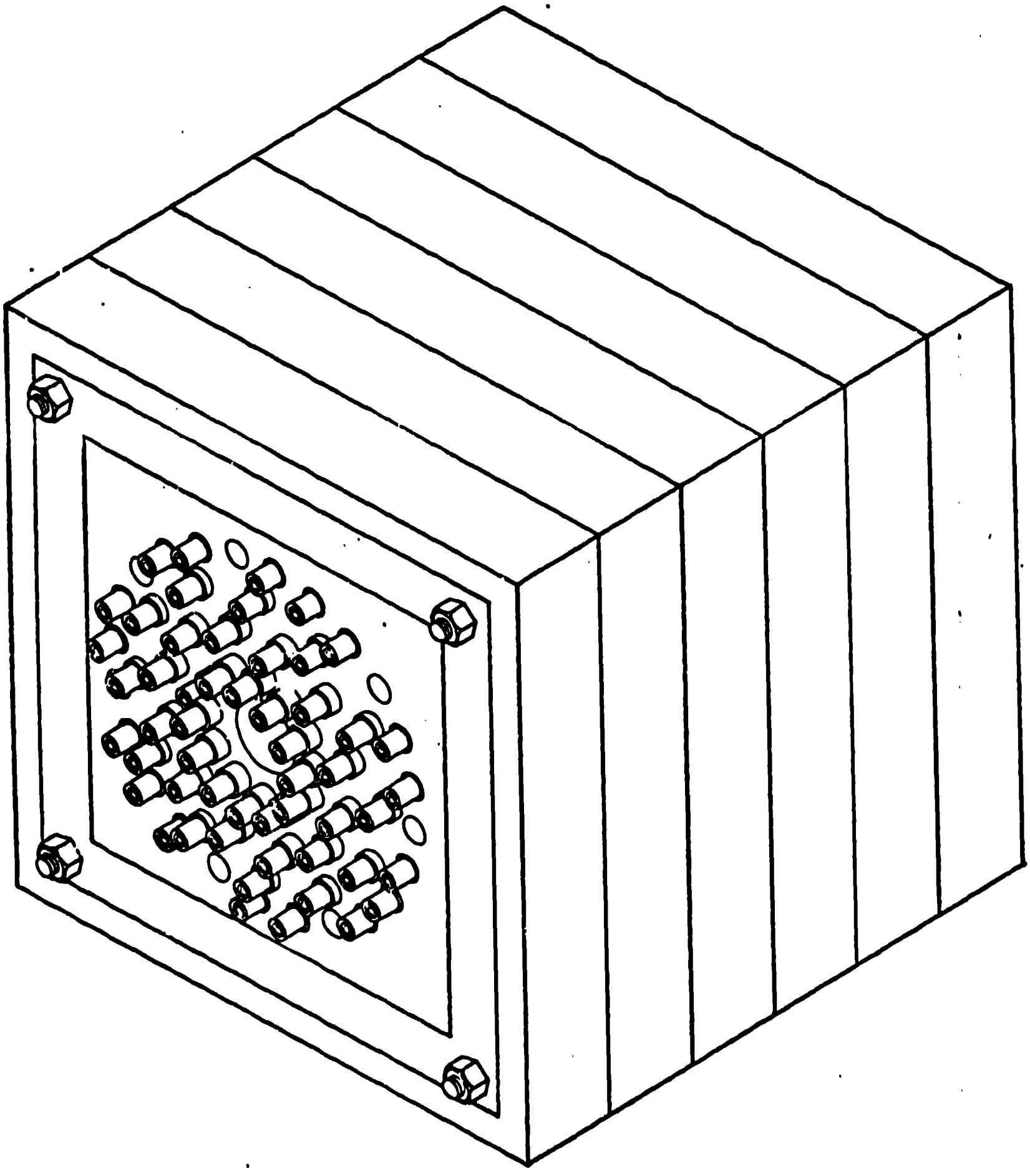

Fig. 1 The Neutron Detector. A 61 cm cube of polythene with 4 rings of 2.54 cm diameter, 61 cm long ^{3}He proportional counter tubes, and a central sample hole. The hole is 3.8 cm in radius, and the tubes are in rings with radii of 6.4-, 10.8-, 14.6-, and 17.8-cm. Fifty-three ^{3}He tubes were used in the work described in this paper.

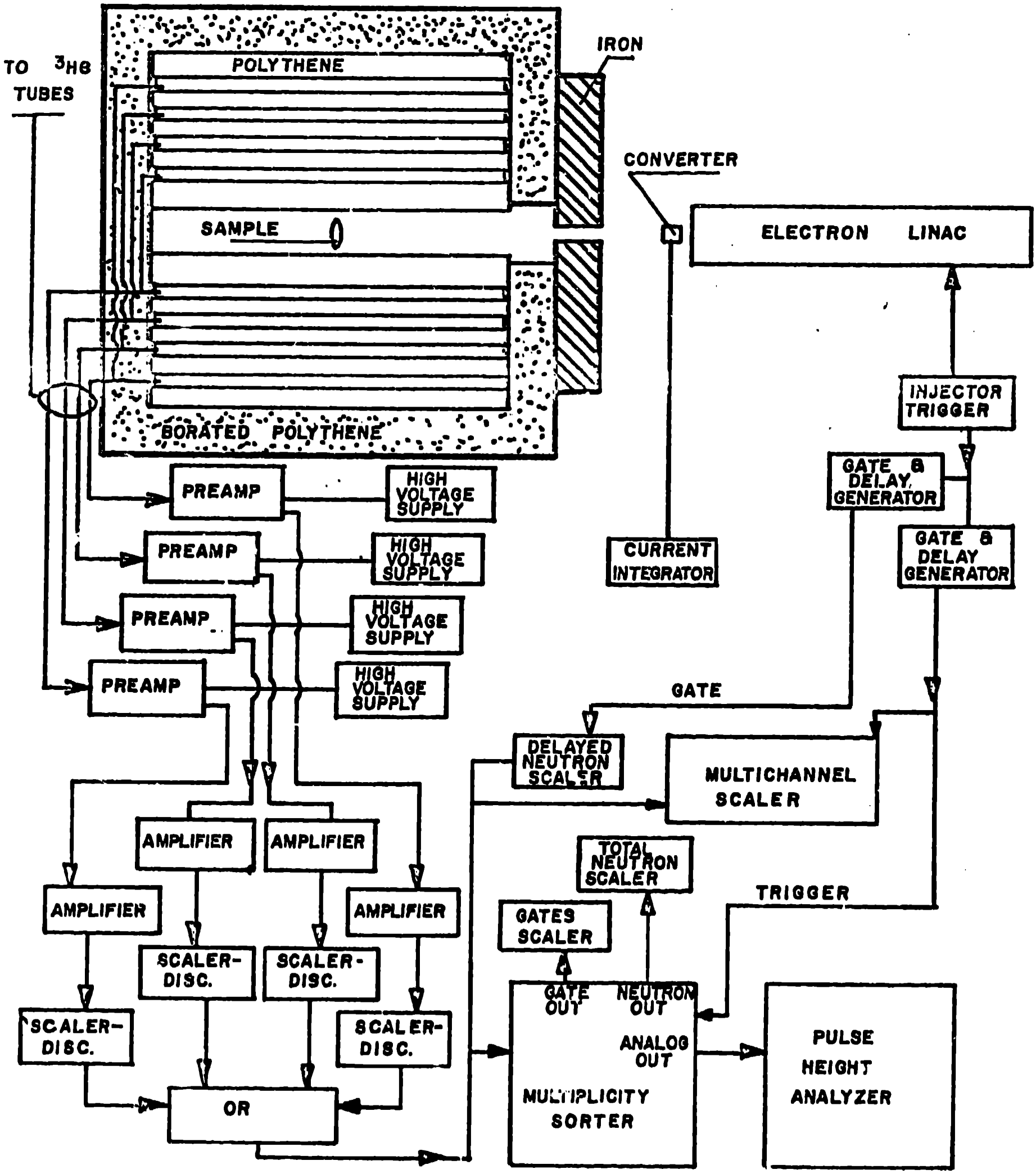

Fig. 2 Block Diagram of the Neutron Detection System

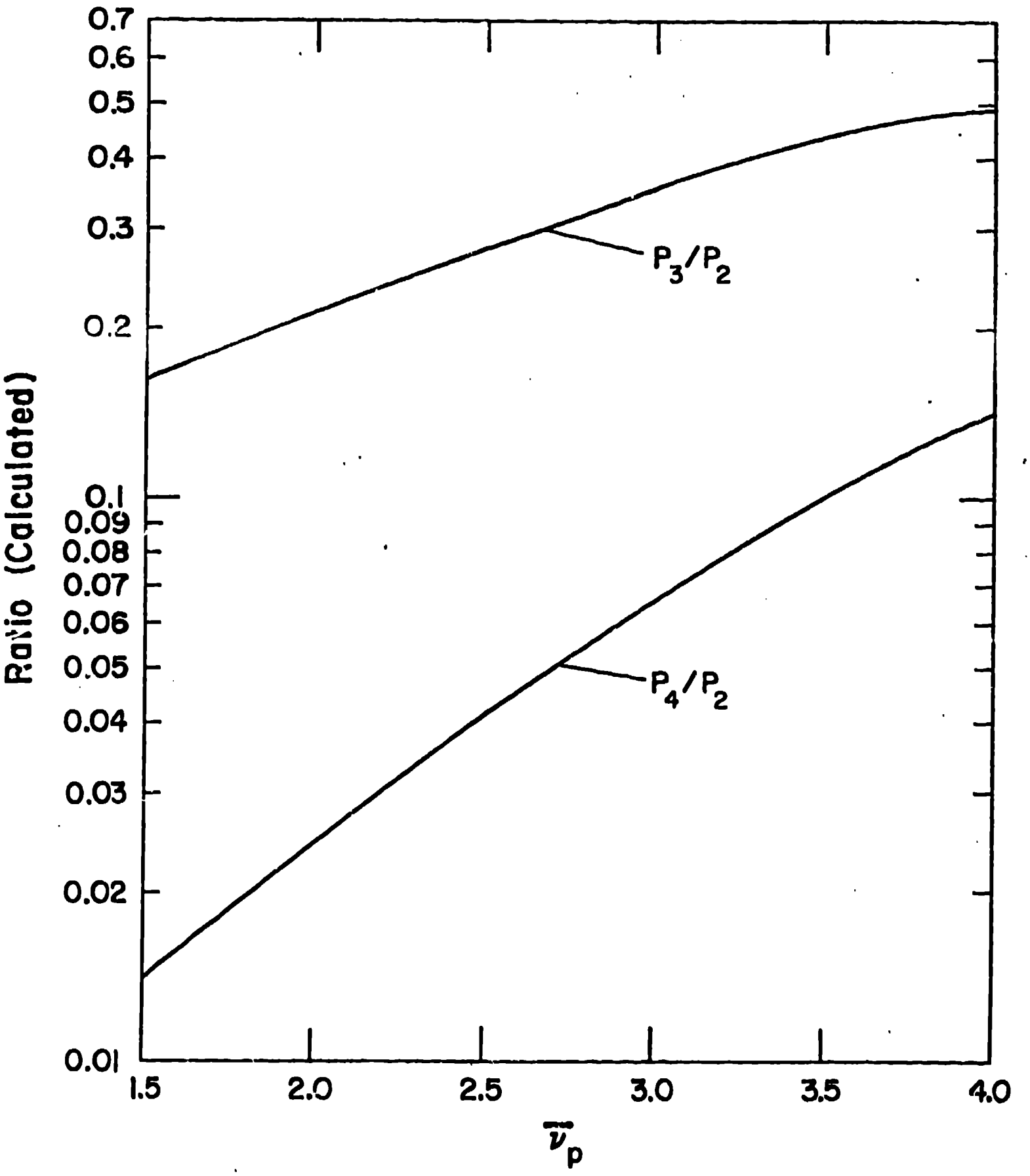

Fig. 3 Typical variation of the ratios of observed multiplicities with $\bar{\nu}_p$ with σ = 1.15 and a typical efficiency.

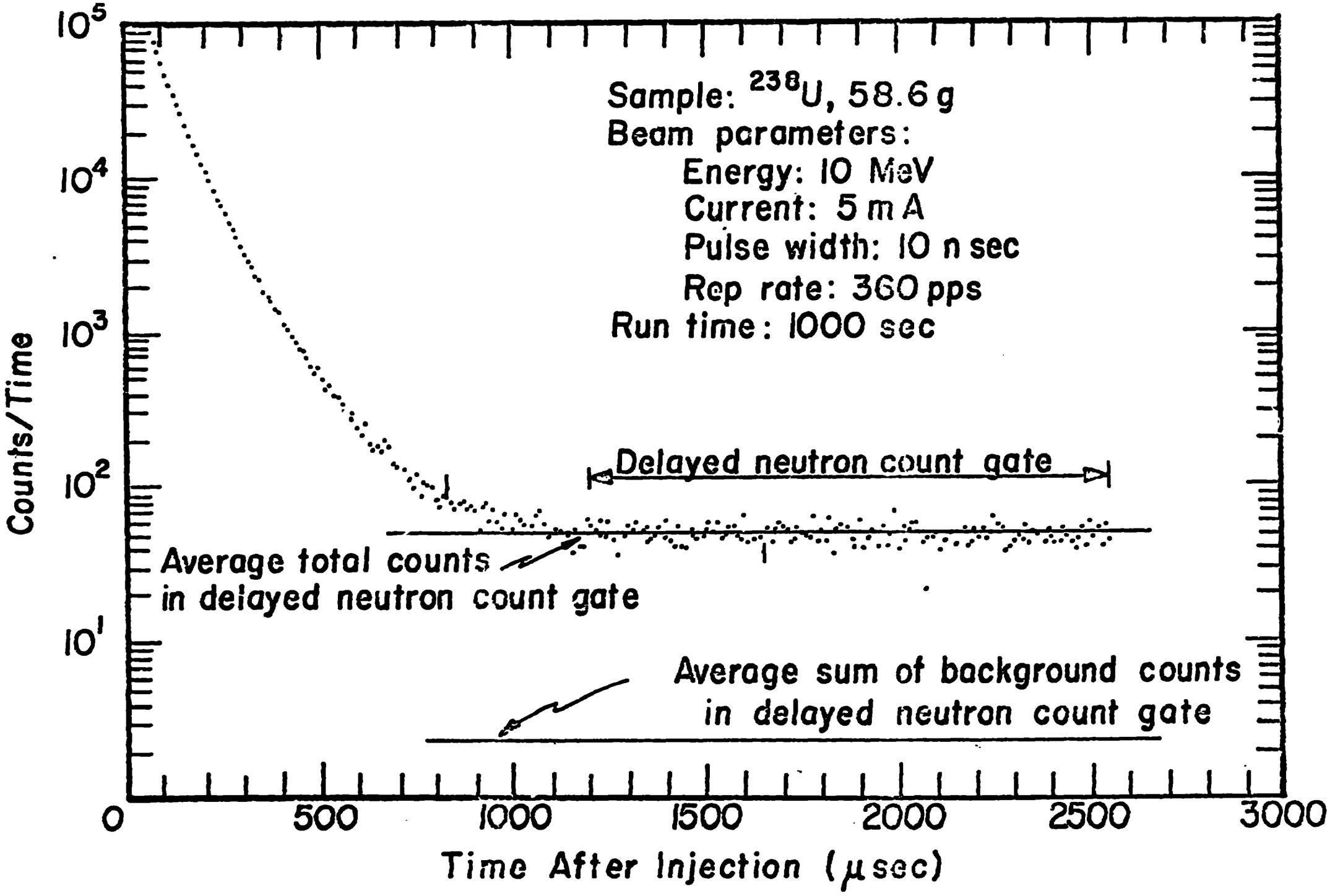

IAEA/SM-174/100

Fig. 4 Time variation of pulses from the Neutron Detector during a typical run.